

A Rational Function Model of Spatial Summation and Single Neuron Computation Based on Equivalent Circuit Models

M. Wang C.N. Zhang

Department of Computer Science, University of Regina
Regina, Saskatchewan, Canada S4S 0A2

Abstract

In this work, neuronal spatial summation is studied by using equivalent circuit models. The whole membrane surface is considered as a pavement of small, nonoverlapping patches. Accordingly, the equivalent circuit model of a cell membrane consists of a set of patch modules interconnected through an axial resistance network. Based on the equivalent circuit model a closed-form formulation for spatial summation is developed. It is demonstrated that the spatial summation follows strictly the rule of weighted-averaging, which essentially prescribes a nonlinear relation between the spatial summation and individual patch electromotive potentials. By considering the transmitter-gated conductances as functions of presynaptic neuronal activities, we develop a rational function model for neuronal interactions. This new model of single neurons affords all four basic arithmetic operations. We show that through suitable, biologically plausible, arrangement of parameters in the proposed model, single neurons can effectively perform complicated nonlinear computations.

Keywords: spatial summation, rational function, equivalent circuit, membrane potential, rational approximation.

1 Introduction

Neuronal integration is a spatiotemporal process in which individual synaptic potentials generated at different sites and different time on a single neuron determine cooperatively whether an action potential is fired. In this work we focus on *spatial summation*, the spatial aspect of neuronal integration. The necessity for spatial summation is usually claimed as that since the postsynaptic potentials produced by individual synapses would suffer a decay before they finally spread to the axon hillock, sufficiently many postsynaptic potentials have to be added together in order to overcome the triggering threshold (Kandel *et al* 1991). Following this understanding, study of spatial summation consists of two basic issues: how individual postsynaptic potentials spread? and how potentials arriving at a specific spatial site are added up?

Most modeling works regarding the first issue have been essentially based on the cable theory (Jack 1979). Depending on the type of cross-membrane channels under consideration, the cable theory has succeeded in solving two classes of problems: generation and conduction of action potentials along the neuronal axon and passive spread of single electrotonic potentials in dendrites (Hodgkin 1964; Jack *et al* 1975). The nature of this method is to consider a segment of axon or dendrite as a one-dimensional cable and to solve the boundary/initial problems concerning the cable equation. An alternative to this continuous approach is to consider a discrete representation of fibers as finite ladder networks. In both cases, a closed-form expression of the cross-membrane potential at a given site is normally available.

Despite its success in modeling the spread of single electrotonic potentials, the cable theory-based approach is not an adequate tool for the modeling of spatial summation. This limitation is intrinsic in the nature of the approach. When multiple synaptic signals are considered, which causes conductance changes at multiple sites in the model network, the principle of superposition is no longer applicable. This difficulty blocks any solution based on linear summation of single-signal solutions. Besides, most cable theory-based methods work

with one-dimensional linear networks. While a dendritic segment can be approximated by a one-dimensional ladder, two-dimensionality seems to be a nature of most problems (e.g. it seems more adequate to define the signal spreading on cell body as a two-dimensional, than a one-dimensional, problem). Compartmental model (Rall 1964; Segev *et al* 1989), which has achieved substantial success in solving dendritic problems, can be viewed as an intermediate approach between pure one-dimensional and pure two-dimensional descriptions. This model basically follows a discretized numerical approach, and does not lead to a closed-form formulation of signal integration.

Although the discrete, numerical calculations provide us with important information about the biophysics and information processing of single neurons, a closed-form function of spatial summation that explicitly interrelates the inputs to and the response of a single neuron is preferable in physiological study. Due to the lack of such a closed-form formulation, a linear summation model for spatial summation has been the most popularly assumed and relied upon in both theoretical and experimental studies (for example, the simple cell model in primary visual cortex, see Hubel and Wiesel 1962). According to this model, the spatial summation is determined by a weighted summation of individual synaptic inputs. An important reason for the popularity of the linear summation model is that it admits the principle of superposition, which provides an efficient way to understand a system's response properties. Despite this, drawbacks with the linear summation model are obvious. Some important experimental facts can not be well accounted for by the linear summation model (for a recent example, see Heeger 1992, 1993). Most critically, it may overlook significant information processing functions conducted by single neurons (for dendritic tree information processing, see Koch and Poggio 1983; Segev and Rall 1988; Mel 1994).

In this work, we work on a closed-form formulation for spatial summation based on membrane equivalent circuit models. A main idea of this work is that, although there have been a number of suggestions that complicated single neuron functions be supported by special membrane mechanisms (Shepherd and Brayton 1987; Koch *et al* 1983; Zador *et al* 1992; Mel 1994), nonlinear single neuron computation can be an intrinsic, universal nature of general membrane structures with parallel conductive channels. In order to tackle two-dimensional problems, different from the compartmental model, we consider the membrane as a pavement of some isopotential patches. In section 2, different patch models are briefly reviewed and a pavement model is described. In section 3, we derive a rational function model for spatial summation. By taking presynaptic activity into consideration, a rational function model for neuronal interaction is derived in Section 4. We shall see that this model endows single neurons with complicated computational power. In Section 5, we discuss possible functional significances of the proposed model. The main purpose of this work is to derive a closed-form formulation of spatial summation and to investigate its possible significance to single neuron computation. In order to focus on this goal, biophysical detail of the underlying membrane mechanisms is not emphasized.

2 Membrane Pavement and Equivalent Circuits

2.1 Models of Single Membrane Patches: A Review

Loosely speaking, a patch refers to an isopotential and spatially local area on a cell's membrane. Even with these two specifications, a membrane patch can still be defined in varied ways. For the purpose of spatial summation study, we understand a patch as a membrane area where all transmitter-gated channels are gated by a single synapse. Neglecting the influence of a presynaptic terminal on distant channels, this description of membrane patch actually refers to the postsynaptic membrane area that is directly opposed to the presynaptic terminal. The local cross-membrane potential in that patch is referred to as the *patch potential*.

Fig.1 collects different electrical models of isopotential membrane patches (see also Table I for a functional classification). These equivalent circuit models proposed with different purposes in different time captured different cross-membrane channel/pathway mechanisms that underlie patch potentials. The most complete model is shown in Fig.1(a) (even though it is claimed to be the most complete, some recently-described channel mechanisms, e.g. the double-gated channels, are not included). The resting nature of the membrane patch is reflected by a constant conductance g_m in series with a fixed electromotive potential E_m . The value of parameter g_m , when conductance channels for ion species 1, 2, ... are considered, is calculated as $g_m = \sum_j g_j$ where g_j is the conductance for the j^{th} ion species (e.g. $g_m = g_{Na} + g_K + g_{Cl}$). E_m , the resting potential, is determined by

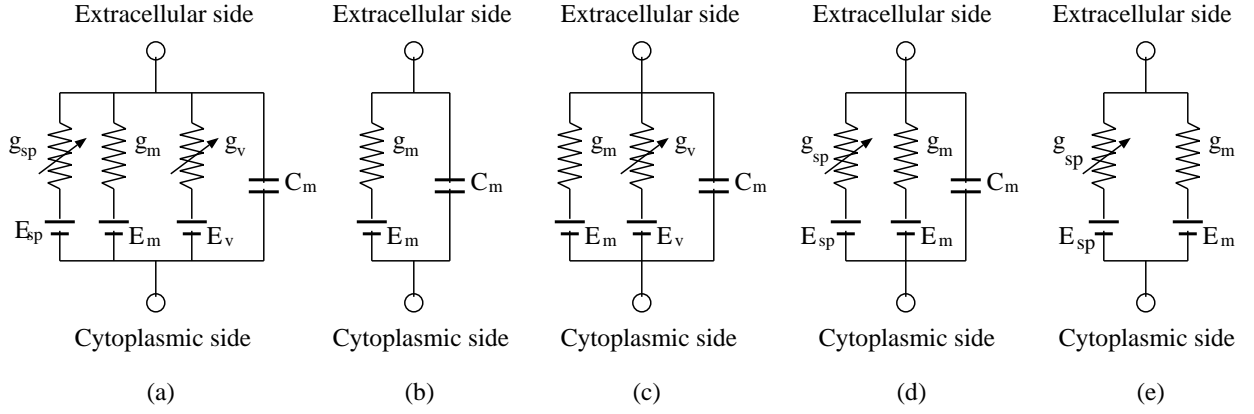


Figure 1: Equivalent circuit models of an isopotential membrane patch. (a) A complete model taking both passive and active properties into consideration, showing the non-gated, voltage-gated, and transmitter-gated ionic channels, and the capacitive pathway. (b) The $g_m - E_m$ branch, in parallel with a capacitance pathway, is usually used as a model for resting properties of a patch. (c) The model with $g_v - E_v$ and $g_m - E_m$ branches and the capacitance pathway in parallel is a building-block of circuit models for action potential conduction. (d) The model used for the study of neuronal integration, where the resting branch $g_m - E_m$, the transmitter-gated branch $g_{sp} - E_{sp}$, and the capacitance pathway, are considered. (e) The model for spatial summation.

a weighted average:

$$E_m = \frac{1}{g_m} \sum_j g_j E_j \quad (1)$$

where E_j is the j^{th} species's Nernst potential. The nature of the resting pathway is that it is only determined by those non-gated cross-membrane ionic channels. In other words, it reflects those constant properties of the membrane patch which is independent of its response to electrical or chemical signals. Operating in parallel with a capacitance pathway (Fig.1(b)), the $g_m - E_m$ pathway provides a model for the resting properties of the patch potential.

TABLE I. MEMBRANE PATCH CIRCUIT MODELS

Model	Channels (pathways) Considered	Applicable Areas	Applications
Fig.1(a)	All non-gated, Voltage-gated, transmitter-gated channels and the capacitance pathway	In theory, all areas	
Fig.1(b)	Non-gated channels and the capacitance pathway	Soma, dendrites	Resting property; passive tangential-membrane conduction of single electrotonic potentials
Fig.1(c)	Voltage-gated channels, non-gated channels, and the capacitance pathway	Axon	Action potential
Fig.1(d)	Transmitter-gated channels, non-gated channels, and the capacitance pathway	Soma, dendrites	Neuronal integration
Fig.1(e)	Transmitter-gated channels and non-gated channels	Soma, dendrites	Spatial summation

There are two gated pathways in the general model. The $g_v - E_v$ pathway describes the voltage-gated ion

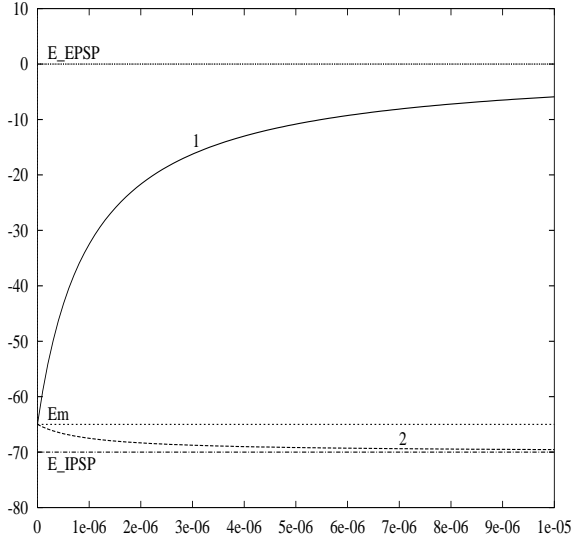


Figure 2: Patch electromotive potential as a function of g_{sp} . Curve 1: V^m when $E_{sp} = E_{EPSP}$; curve 2: V^m when $E_{sp} = E_{IPSP}$. g_m is set to $1 \times 10^{-6} S$.

channels in the patch. This pathway is necessary for the patches where the voltage-gated channels are abundant (e.g. the axon patches). The conductance g_v is a variable determined by the cross-patch potential. The $g_{sp} - E_{sp}$ branch reflects the transmitter-gated channel mechanism, where g_{sp} is a function of synaptic efficacy as well as of presynaptic activity. E_{sp} is the reversal potential of synaptic potential, that is, $E_{sp} = E_{EPSP}$ for excitatory patches and $E_{sp} = E_{IPSP}$ for inhibitory patches.

To focus on spatial summation, in the rest of this work we consider peak steady-state values of patch potentials, which means that the capacitive current is null. Under this circumstance the capacitor C_m in the equivalent circuits will be omitted. Fig.1(e) shows such a model which serves as a building-block for equivalent circuit models of spatial summation. We also ignore temporal summation effect by assuming that all patch potentials reach their peak values at the same time. The patch model in Fig.1(e) has a *patch electromotive potential*

$$V^m = \frac{g_m E_m + g_{sp} E_{sp}}{g_m + g_{sp}} \quad (2)$$

which is a weighted average of the resting potential E_m and the reversal potential E_{sp} . It is worth noting that the patch electromotive potential is a nonlinear (rational) function of g_{sp} . This rational function has a zero at $g_{sp}^0 = -g_m E_m / E_{sp}$ and no pole because $g_m > 0$ and $g_{sp} \geq 0$. The graph of this function is an equilateral hyperbola (Fig.2). With small g_{sp} values the gated channels have little contribution to the patch electromotive potential and the value of V^m approximates E_m , the resting potential; when the gated channels dominate the non-gated channels ($g_{sp} \gg g_m$), V^m approaches to E_{sp} , the reversal potential of the gated electromotive potential.

2.2 Membrane Pavement

The membrane patch models outlined above describe *cross-membrane* electrical activities, being it the resting, synaptic, or action potentials, in a single membrane patch. To a large extent, spatial summation is a *tangential-membrane* activity where synaptic potentials spread and integrate from patches to patches. To model this tangential-membrane phenomenon we consider the whole membrane surface, excluding the axon, of a single neuron as a segmentation, or a *pavement*, by membrane patches. Specifically, when spatial summation is focused,

only patch models given in Fig.1(b) and (e) are used for the pavement. By doing so we are aware that those active properties due to voltage-gated membrane mechanisms are ignored. A patch of the form Fig.1(b) paves a local area on the membrane where transmitter-gated channels are rare, and a patch given in Fig.1(e) can pave the area underneath a single synapse. To unify the description, we may consider a pavement strategy in which only the patch model in Fig.1(e) is used: if the gated channels in a patch can be neglected, the g_{sp} there is set to zero. In the rest of this work we shall follow this convention.

Tangential-membrane interactions among patches are modeled by an *axial resistance network*. If the tangential-membrane current between patch i and patch j is significant, then an axial resistance r_{ij} is considered in the network which connects the equivalent circuits of patch i and patch j . Fig.3 illustrates equivalent circuits corresponding to different pavement geometry. In building our equivalent circuit models, the extracellular environment is supposed to be of low resistance so that the extracellular side of the circuit is equipotential and is represented by a short-circuit. Furthermore, the resting property of membrane is assumed uniform throughout all patches so that the values of g_m and E_m are the same everywhere.

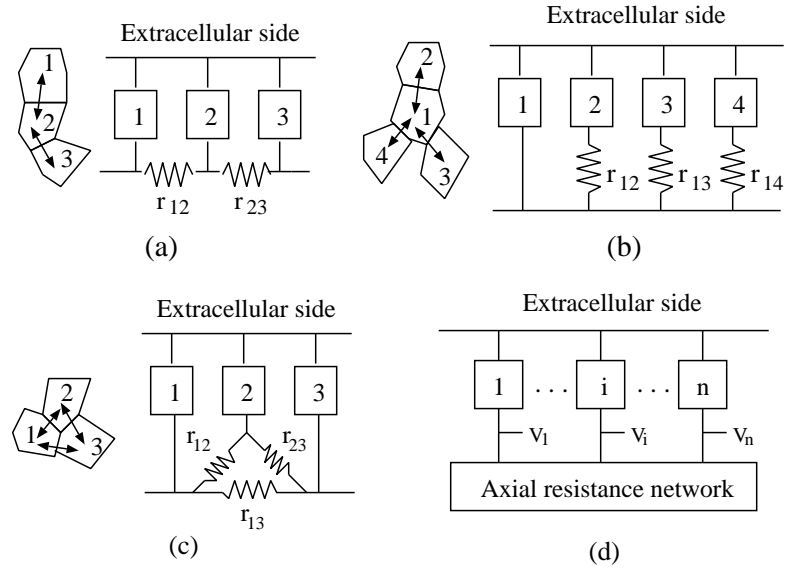


Figure 3: (a) - (c) Equivalent circuits corresponding to different pavement geometry. Each numbered box stands for a patch model as shown in Fig.1(e). Bidirectional arrows in the figures indicate unnegligible tangential-membrane ionic flows between adjacent patches. (d) The most general circuit model corresponding to arbitrary pavement strategy. Patch potentials are measured at points V_1, V_2, \dots, V_n .

It is worth noting that the equivalent circuit for a given membrane is usually not unique, depending on how the axial resistance network is configured. Although the theoretical number of possible axial resistances for an n -patch pavement is $n(n - 1)/2$, a notable feature of axial resistance network is its local connectivity, which makes the actual axial network much simpler with a few, local, connections.

3 A Rational Function Model for Spatial Summation

Once a membrane pavement is given, tangential-membrane activity can be studied through the corresponding equivalent circuit model. The definition of patch electromotive potential given in (2) can be generalized to those patch modules in the general circuit model in Fig.3(d): let V_i^m be the electromotive force of patch i . It is measured at the site of V_i in Fig.3(d) when patch i is isolated from the axial resistance network, and is evaluated according to relation (2).

3.1 Spatial Summation Theorem

Consider an arbitrary n -patch pavement as shown in Fig.3(d). The spatial summation at patch i , denoted as V_i , is the cross-membrane potential observed at patch i when it is connected with the axial resistance network. In respect to the axial resistance network, if V_i^m is the *open-circuit* patch potential at patch i , then V_i is the *closed-circuit* patch potential. According to Kirchhoff's fundamental rules for linear circuits, V_i is measured as the total ionic flow from all patches to the considered patch divided by the total conductance. Define the *inter-patch conductance* G_{ij} as

$$G_{ij} = [(g_m + g_j)^{-1} + R_{ij}]^{-1}, \quad (3)$$

which is the conductance of patch j in series with the conductance resistance R_{ij} evaluated in the configuration in Fig.4, we have the following basic theorem of spatial summation:

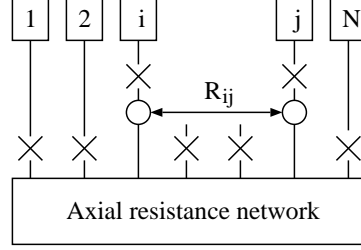


Figure 4: The measurement of R_{ij} .

Theorem In an n -patch membrane pavement with arbitrary axial resistance network, the spatial summation value at any patch i is the weighted average of the patch electromotive potential of all patches, with the weighting factors given by the inter-patch conductances calculated from all individual patches to the patch i , respectively. Let V_i be the spatial summation at patch i , V_j^m be the electromotive potential of patch j , and G_{ij} be the inter-patch conductance between patches j and i , We have

$$V_i = \frac{1}{\sum_j^n G_{ij}} \sum_j^n G_{ij} \times V_j^m \quad (4)$$

In regard to the relation between patch electromotive potentials and spatial summations, equation (4) describes a weighted-averaging model for spatial summation. However, for the relation between individual gated conductances and spatial summations, equation (4) defines a *rational function* model for spatial summation. In fact, by substituting (2) and (3) into (4), one has

$$V_i = \frac{\sum_j [E_m g_m + E_j g_j] \prod_{k \neq j} [1 + R_{ik}(g_m + g_k)]}{\sum_j [g_m + g_j] \prod_{k \neq j} [1 + R_{ik}(g_m + g_k)]}. \quad (5)$$

In this expression, the spatial summation V_i is represented as a rational function of the gated conductances g_1, g_2, \dots, g_n : both the numerator and the denominator of (5) are polynomials of the n^{th} -degree concerning g_1, g_2, \dots, g_n . The degree of the polynomials in g_j ($j = 1, 2, \dots, n$) is one. All coefficients, with the possible exception of E_j , are positive constant. The sign of E_j is determined by the selection of E_m . If E_m is chosen as zero, then $E_j > 0$ when $E_j = E_{EPSP}$ and $E_j < 0$ when $E_j = E_{IPSP}$. Fig.5 shows the pictures of the rational function model (5) for $n = 2$ (a two-patch pavement).

3.2 Monotony, Saturability, and the Isopolar Neighbor Shunting

The rational function (5) has a number of important properties. We first point out that V_i is an increasing (or decreasing) function of g_j , $j = 1, 2, \dots$ if $E_j = E_{EPSP}$ (or E_{IPSP}). From the basic theorem (4) we know that $\partial V_i / \partial V_j^m = G_{ij} / (\sum G_{ij}) > 0$, which means that V_i is an increasing function of patch electromotive potentials. We also have that, from (2), $\partial V_j^m / \partial g_j = g_m (E_j - E_m) / (g_m + g_j)^2$. Therefore, V_j^m is an increasing function of g_j when $E_j > E_m$ (i.e. when $E_j = E_{EPSP}$) and a decreasing function when $E_j < E_m$ (i.e. when $E_j = E_{IPSP}$).

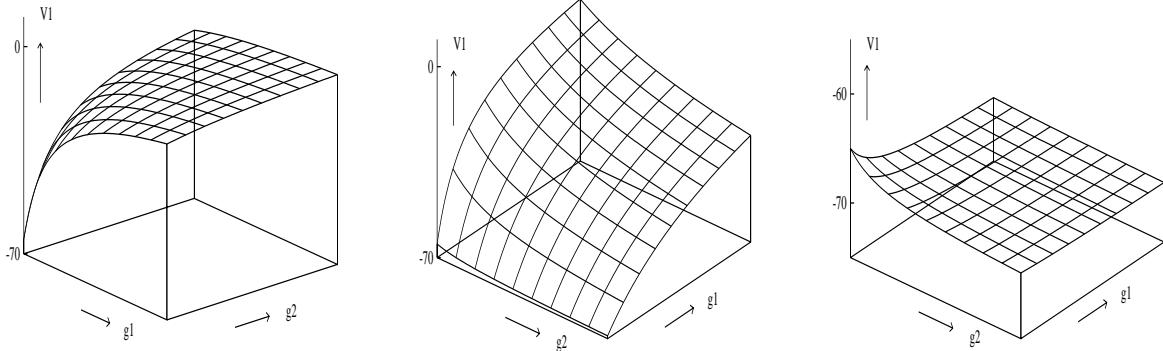


Figure 5: Pictures of the rational function model with $n = 2$. Left: $E_1 = E_2 = E_{EPSP}$. Middle: $E_1 = E_{EPSP}$ and $E_2 = E_{IPSP}$. Right: $E_1 = E_2 = E_{IPSP}$. For all pictures, g_1 and g_2 change from 0 to $5 \times 10^{-5} S$. V_1 is the spatial summation observed at patch 1.

The monotonicity of the rational function (5) assures us that in an arbitrary membrane pavement, the contribution of an excitatory (inhibitory) gated conductance to the spatial summation is always positive (negative). Meanwhile, spatial summation saturates itself for large-valued gated conductances. This is implied by that both the numerator and the denominator of (5) are of the same degree concerning a specific g_j . To estimate the upper and lower bounds to the value of V_i , we notice that, from (4),

$$\min\{V_1^m, V_2^m, \dots, V_n^m\} \leq V_i \leq \max\{V_1^m, V_2^m, \dots, V_n^m\}. \quad (6)$$

Since the relation (2) requires that

$$\begin{aligned} E_m \leq V_j^m < E_j, & \quad \text{if } E_j = E_{EPSP}, \\ E_m \geq V_j^m > E_j, & \quad \text{if } E_j = E_{IPSP}, \end{aligned}$$

We have a looser relation:

$$\min\{E_m, E_1, E_2, \dots, E_n\} \leq V_i \leq \max\{E_m, E_1, E_2, \dots, E_n\}. \quad (7)$$

An even looser estimator is that

$$E_{IPSP} < V_i < E_{EPSP}. \quad (8)$$

The monotonicity of the rational function (5) implies that the contributions of several excitatory patches are always accumulative. However, it does not imply that when several excitatory patches interact, the value of spatial summation at a specific patch has to be larger than its patch electromotive potential. Let us take as example a two-patch system, with $E_1 = E_2 = E_{EPSP}$, and consider V_1 and V_2 , the spatial summation at the two patches, respectively. If $g_1 < g_2$, which implies that $V_1^m < V_2^m$ by (2), we have $V_1^m < V_1 < V_2^m$ and $V_1^m < V_2 < V_2^m$ by (6). That is, the value of spatial summation at patch 1 is larger than the value of the electromotive potential at patch 1; however, the value of spatial summation V_2 is lower than its patch electromotive potential due to the existence of a closely-sited, less active, excitatory patch. Similarly, for two inhibitory patches, if $g_1 < g_2$, which implies that $V_1^m > V_2^m$, we have $V_1^m > V_1 > V_2^m$ and $V_1^m > V_2 > V_2^m$.

In this case, the value of spatial summation at patch 2 is higher, instead of lower, than its patch electromotive potential, with an inhibitory but less active neighborhood.

To summarize, if we regard the open-circuit patch potential V_i^m as the contribution of channels g_m and g_i to V_i in the absence of other patches, then the phenomenon described above states that a neighboring patch j ($j \neq i$) whose gated mechanism is less active but with the same polarity (that is, $E_i = E_j$) would act in effect against the V_i^m .

This is an inhibition mechanism different from the inhibition observed between oppositely-polarized patches, and is due to the existence of the non-gated conductance g_m . In the case of oppositely-polarized patches, the inhibition mechanism is implemented by a current-shunting effect imposed by the inhibitory patch on the excitatory patch. In the weighted-averaging relation (2), E_m and E_{sp} are two ‘forces’ influencing the V^m : each of them tends to make the value of V^m closer to itself and away from the other. In this sense, E_m and E_{sp} always counteract each other whatever type the E_{sp} is. Take V_1 as example: putting patch 2 next to patch 1 would not only contribute a gated conductance g_2 but also a new E_m which counteracts E_1 . It is the combination of g_m and g_2 that determines the contribution of V_2^m to V_1 . Suppose $E_1 = E_2 = E_{EPSP}$ (the following comments applies to the case of $E_1 = E_2 = E_{IPSP}$ as well). When $g_1 > g_2$, which means that $V_1^m > V_2^m$, we have a net tangential-membrane current I_{12} flowing from patch 1 to patch 2 (see Fig.6). Because I_{12} shunts the current I_{sp} , it causes a loss of potential drop across g_1 , which results in $V_1 < V_1^m$.

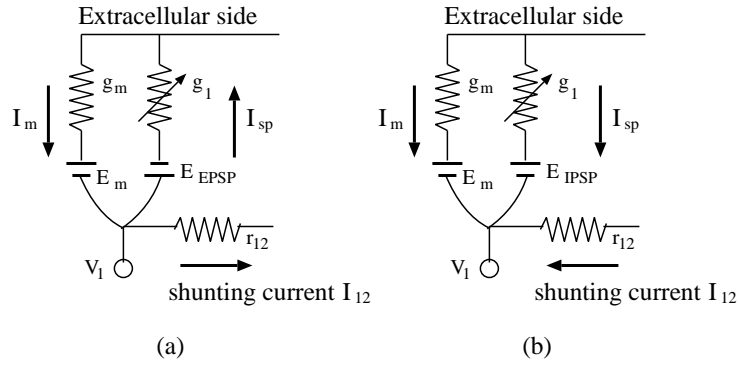


Figure 6: Two kinds of isopolar neighbor shunting ($g_1 > g_2$). (a) When patches 1 and 2 are both excitatory and $g_1 > g_2$, there is a net tangential-membrane current I_{12} from patch 1 to patch 2, which shunts I_{sp} at patch 1. (b) When patches 1 and 2 are both inhibitory and $g_1 > g_2$, there is a net tangential-membrane current I_{12} from patch 2 to patch 1, which still shunts I_{sp} at patch 1.

This observation can be generalized to several adjacent patches with the same polarity. For several closely-sited, isopolar patches, the spatial summation at a given patch would suffer a remarkable loss in magnitude if only a few (including itself) gated conductances are active while most of others are much less active. Since the shunting effect is significant when r_{12} is small and happens for isopolar patches, the phenomenon can be referred to as *isopolar neighbor shunting*. Table II lists all possible relations between spatial summation and open-circuit patch potential for two-patch systems. It can be seen that the normal inhibition (when $E_1 \neq E_2$) is unrelated with the comparison between g_1 and g_2 .

TABLE II. RELATIONS BETWEEN V AND V^m

E_1	E_2	$g_1 > g_2$	$g_1 < g_2$
E_{EPSP}	E_{EPSP}	* $V_1 < V_1^m$, $V_2 > V_2^m$	$V_1 > V_1^m$, * $V_2 < V_2^m$
E_{EPSP}	E_{IPSP}	** $V_1 < V_1^m$, $V_2 > V_2^m$	** $V_1 < V_1^m$, $V_2 > V_2^m$
E_{IPSP}	E_{EPSP}	$V_1 > V_1^m$, ** $V_2 < V_2^m$	$V_1 > V_1^m$, ** $V_2 < V_2^m$
E_{IPSP}	E_{IPSP}	* $V_1 > V_1^m$, $V_2 < V_2^m$	$V_1 < V_1^m$, * $V_2 > V_2^m$

Note: * Isopolar neighbor shunting; ** Normal inhibition.

3.3 Axial Resistance Networks

In comparison with the neat relationship between V_i and the gated conductances, the influence of axial resistances on V_i is subtle. If we consider (5) as a function between V_i and R_{ij} 's, then it is also a rational function. A plain fact is that V_i saturates itself for large R_{ij} 's. Besides this, the monotonicity of this function is uncertain. In fact, from (3) one has that G_{ij} is a decreasing function of R_{ij} , but from (4) the sign of

$$\partial V_i / \partial G_{ij} = \sum_k G_{ik} (V_j^m - V_k^m) / [\sum_k G_{ik}]^2$$

is undetermined.

For the two-patch systems, where r_{12} is the only axial resistance connecting the two patches, the influence of r_{12} on V_1 is depicted in Fig.7. A common property shared by all curves is that the contribution of the gated conductance (g_2) to V_1 decays as r_{12} increases. On the left end ($r_{12} = 0$) of each curve V_1 is simply the weighted average of the two patch electromotive potentials, the weighting factors being the two patch conductances. On the right hand side of each curve, the value of V_1 approaches to V_1^m as r_{12} increasingly blocks the contribution of V_2^m .

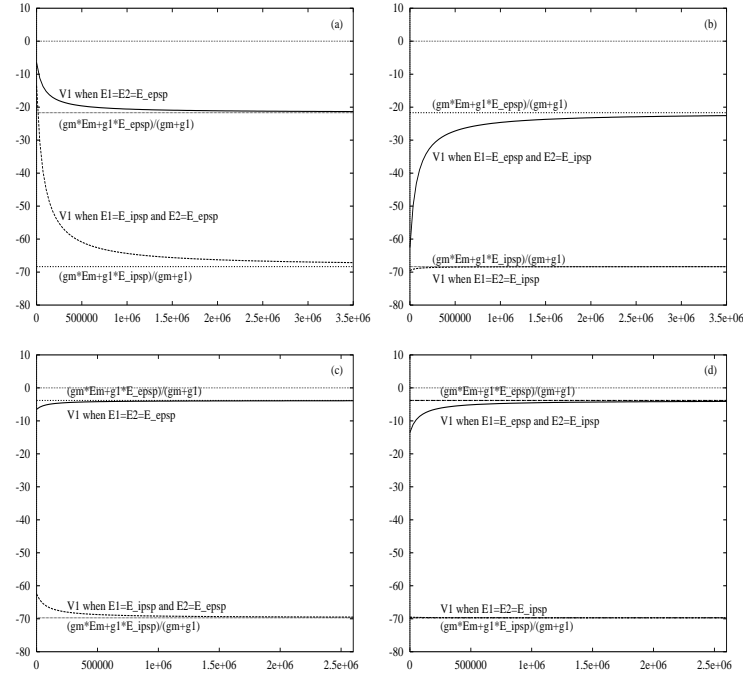


Figure 7: V_1 vs r_{12} curves. Upper figures: $g_1 < g_2$; lower figures: $g_1 > g_2$. (a) $E_2 = E_{EPSP}$; (b) $E_2 = E_{IPSP}$; (c) $E_2 = E_{EPSP}$; (d) $E_2 = E_{IPSP}$. Parameters for all figures: $g_m = 5 \times 10^{-6} S$, $E_m = -65 mV$, $E_{EPSP} = 0 mV$, $E_{IPSP} = -70 mV$. For upper figures: $g_1 = 1 \times 10^{-5} S$, $g_2 = 8 \times 10^{-5} S$. For lower figures: $g_1 = 8 \times 10^{-5} S$, $g_2 = 1 \times 10^{-5} S$.

In the case of $g_1 < g_2$, that is, when the farther synapse contributes more than the nearer synapse, V_1 approaches to V_1^m from above the V_1^m when $E_2 = E_{EPSP}$ (see Fig.7(a)), and from below the V_1^m when $E_2 = E_{IPSP}$ (Fig.7(b)). This observation fails to be generalized to the case of $g_1 > g_2$. As can be seen from Fig.7(c),(d), the curve V_1 when $E_1 = E_2 = E_{EPSP}$ in (c) and the cure V_1 when $E_1 = E_2 = E_{IPSP}$ in (d) behave just the opposite as they do in Fig.7(a), (b): V_1 approaches to V_1^m from below when both E_1 and E_2 are E_{EPSP} , and from above when both are E_{IPSP} . These two curves illustrate the effect of isopolar neighbor shunting.

One-dimensional pavements can be applied to dendrites and give rise to certain ladder circuits. The evaluation of axial resistances in a ladder network becomes especially simple. The R_{ij} between patch i and patch j is simply a summation (assume $i < j$):

$$R_{ij} = r_{i,i+1} + r_{i+1,i+2} + \dots + r_{j-1,j}.$$

For simplicity we assume that all axial resistances possess the same value of r_a , which makes $R_{ij} = |j - i|r_a$. Suppose the number of patches in the ladder is n , we first consider the spatial summation V_i at patch i , $1 \leq i \leq n$, with the only one nonzero g_λ at patch λ , $1 \leq \lambda \leq n$. We have:

$$V_i = \frac{E_\lambda g_\lambda}{g_m + g_\lambda + g_m[1 + |\lambda - i|r_a(g_m + g_\lambda)] \sum_{j \neq \lambda}^n (1 + |j - i|r_a g_m)^{-1}} \quad (9)$$

where the expression $\sum_{j \neq \lambda}^n (1 + |j - i|r_a g_m)^{-1}$ can be effectively evaluated in term of the *psi* function. Similarly, V_i with two nonzero gated conductances g_α and g_β is given by (assume $\alpha \neq \beta$ and $1 \leq \alpha, \beta \leq n$)

$$V_i = \frac{E_\alpha g_\alpha [1 + |\beta - i|r_a(g_m + g_\beta)] + E_\beta g_\beta [1 + |\alpha - i|r_a(g_m + g_\alpha)]}{\left\{ \begin{array}{l} (g_m + g_\alpha)[1 + |\beta - i|r_a(g_m + g_\beta)] + (g_m + g_\beta)[1 + |\alpha - i|r_a(g_m + g_\alpha)] + \\ g_m[1 + |\beta - i|r_a(g_m + g_\beta)][1 + |\alpha - i|r_a(g_m + g_\alpha)] \sum_{j \neq \alpha, j \neq \beta}^n (1 + |j - i|r_a g_m)^{-1} \end{array} \right\}} \quad (10)$$

These equations actually give the distribution of spatial summation values along the one-dimensional pavement. Fig.8 shows some calculation results for the cases of single nonzero g_{sp} and two nonzero g_{sp} 's.

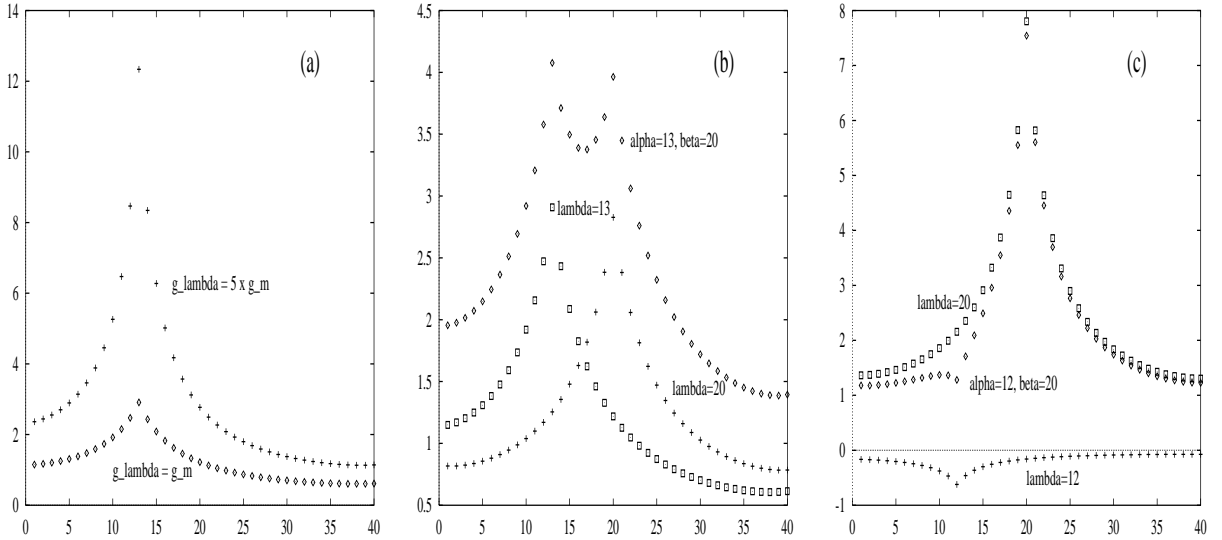


Figure 8: Distributions of spatial summation values over finite ladder networks (40 patches). (a) With only one nonzero g_λ at patch $\lambda = 13$, the distribution of V_i , $i = 1, 2, \dots, 40$ follows a negative exponential law. (b) Spatial summation distribution with two nonzero gated conductances, g_α and g_β , with $\alpha = 13, \beta = 20$, and $E_{13} = E_{20} = E_{EPSP}$. The influences of single gated conductance are also shown. Notice that the spatial summation with two nonzero gated conductances does not strictly follow the rule of superposition. (c) Spatial summation distribution with two nonzero gated conductances, g_α and g_β , with $\alpha = 12, \beta = 20$, $E_{13} = E_{IPSP}$, and $E_{20} = E_{EPSP}$. The influences of single gated conductance are also shown. Parameters for all pictures: $E_m = 0$, $E_{EPSP} = 65$ mV, $E_{IPSP} = -5$ mV, $g_m = 10^{-6}$ S. For (b): $g_\lambda = g_\alpha = g_\beta = g_m$. For (c): $g_\lambda = g_\alpha = g_\beta = 3 \times g_m$.

4 Nonlinear Neuronal Interactions

Spatial summation carried out by tangential-membrane activity directly underlies interactions between neurons. In this section we derive a new neuronal interaction model based on the rational function model for spatial summation.

4.1 Neurons That Add, Multiply, and Divide

Consider a single cortical neuron i and all of its presynaptic neurons $j, j = 1, 2, \dots, n; j \neq i$. According to the membrane pavement model, we may pave the membrane of neuron i with all patches $j, j = 1, 2, \dots, n$ where the j th patch corresponds to synapse j made by neuron j , together with those patches $j, j = n + 1, \dots, N$ with no transmitter-gated channels. The set of spatial summation values $\{V_{i1}, \dots, V_{ij}, \dots, V_{iN}\}$ defines the state of neuron i . Specifically, let the patch at the axon hillock be named h , the spatial summation be V_{ih} . The firing or the output of neuron i , denoted as O , is determined by V_{ih} . Thus, when we write $O(x_i)$ to indicate how the state of a neuron determines its output, we understand that x_i refers to V_{ih} .

We now take the presynaptic activity into consideration. For simplicity, the relation between the transmitter-gated conductance g_j and presynaptic activity $O(x_j)$ is modeled as

$$g_j = \gamma_j \zeta_j O(x_j) = w_j^* O(x_j) \quad (11)$$

where $\gamma_j = dr_j/dO(x_j)$ measures the transmitter releasing efficacy of the presynaptic terminal, r_j being the release intensity of transmitters in the synapse j as a function of $O(x_j)$; the coefficient $\zeta_j = dg_j/dr_j$ reflects the postsynaptic conductance change as a response to transmitter releasing. $w_j^* = \gamma_j \zeta_j$ can be regarded as the *strength* of synapse j . Since the property of synapse j (being excitatory or inhibitory) has been taken into account in the sign of E_j , we hereby take $w_j, j = 1, 2, \dots, n$ as unsigned numbers (notice that in (11) the action of a neuron exerts on another neuron is modeled by a single membrane patch, which is a highly simplified treatment. A neuron can potentially make dozens of synapses on another neuron. If the spatial distribution of those synapses are to be considered, the resultant model of neuronal interaction would become more subtle).

Given relations (5) and (11), the spatial summation $x_i = V_{ih}$ can be evaluated as

$$x_i = \frac{\sum_j [E_m g_m + E_j w_j^* O(x_j)] \prod_{k \neq j} [1 + R_{hk}(g_m + w_k^* O(x_k))]}{\sum_j [g_m + w_j^* O(x_j)] \prod_{k \neq j} [1 + R_{hk}(g_m + w_k^* O(x_k))]} \quad (12)$$

Notice that this relation defines the state of the postsynaptic neuron, x_i , as a rational function of the outputs of presynaptic neurons, $O(x_1), \dots, O(x_n)$. Therefore, it can be regarded as a rational function model for neuronal interactions.

Almost all discussions made in the last section on spatial summation can be readily applied to neuronal interactions. For example, the model requires that x_i do not take values of arbitrary magnitude but saturate itself for large-valued input. Perhaps the most notable feature of the rational function model (12) is its potential in affording complicated computations. As can be seen from (12), all four basic arithmetic operations, including addition, subtraction, multiplication, and division, are involved in single-cell processing of presynaptic neuronal activities. We now discuss how this potential of single-neuron complicated computation can be put into effective through suitable, biologically plausible, arrangement of parameters in the general model.

4.2 Reduce to Linear Summation Model

If $R_{hj}(g_m + w_j^* O(x_j)) \ll 1$ for all j 's, the general relation (12) is reduced to:

$$x_h \approx \frac{\sum_j [g_m E_m + E_j \gamma_j \zeta_j O(x_j)]}{\sum_j [g_m + \gamma_j \zeta_j O(x_j)]} \quad (13)$$

With a *small-signal assumption*:

$$g_m \gg n^{-1} \sum_j g_j, \quad (14)$$

the equation (13) becomes:

$$x_h \approx E_m + \sum_j \left(\frac{E_j}{ng_m} \right) \gamma_j \zeta_j O(x_j). \quad (15)$$

If we further define

$$w_j \equiv \left(\frac{E_j}{ng_m} \right) \gamma_j \zeta_j, \quad (16)$$

and set $E_m = 0$ as the reference for all voltage values, we have

$$x_h \approx \sum_j w_j O(x_j). \quad (17)$$

This is the linear summation model which has been popularly cited and relied upon in most of experimental and theoretical studies.

From the derivation above one can conclude that the linear summation model (17) is an approximation to the rational function model (12) under the condition that $R_{hj}(g_m + w_j^* O(x_j)) \ll 1$ for all j 's and the small-signal assumption (14). This approximation neglects two important natures of the general model and henceforth goes farther away from biological realism. First, we notice that in the general model (5) the axial resistances are always multiplied with patch conductances, which typically results in a product of order 10^0 ($M\Omega \times 10^{-6}S$). As the term $(g_m + w_j^* O(x_j))$ has a lower bound g_m , the only possibility that $R_{hj}(g_m + w_j^* O(x_j)) \ll 1$ is when R_{hj} is small. Even if this is true for those patches close to patch h (the hillock), it is hardly met by those distant patches (say, most dendritic patches). Neglecting all axial resistances equalizes spatial summations at all patches and therefore yields a single spatial summation value for a given cell.

Another problem with the linear summation model is the small-signal assumption, because of which the variable part of the divisor in formula (13) is omitted. In comparison to the small R_{hj} assumption, the small-signal assumption is not hardly satisfied. To understand this we notice that relation (14) prescribes a restriction over the entire membrane rather than at a single patch. If only a small fraction of gated channels are open, then there are a small number of nonzero items in the summation $\sum_j g_j$. With an n enough large, the inequality can be satisfied by those few channels even with large values. As an estimate, let $n = 10^4$, $g_m = 10^{-6}S$. If there are 100 nonzero gated conductances (a fraction of 1% of the total) each of which has a mean value of 10^{-5} (10 times g_m), then the value of g_m is still 10 times the averaged total of gated conductances. Compared with the general model (5), a main loss in the linear model is the nature of saturation for large-magnitude inputs.

Despite those problems, the linear summation model have still found its application in many problems. It does capture the basic nature that presynaptic activities are somehow accumulated. An important property of the linear summation model is that the principle of superposition applies, which is a useful property for stimulus design in some physiological experiments.

4.3 Nonlinear Operation: Division

Recently Heeger *et al* suggested a normalization model for simple cells in primate visual cortex (Heeger 1992; Carandini and Heeger 1994). According to this model, simple cell's response begins with a linear stage, which performs essentially the same function as in the linear summation model, followed by a normalization stage (Fig.9(a)). At the normalization stage, each cell's linear response is divided by a quantity proportional to the pooled activity of other cortical cells (Heeger 1992; Carandini *et al* 1994). The mechanism underlying the normalization model has been investigated (Carandini *et al* 1994) in terms of equivalent circuit model of a cellular membrane (see Fig.9(b)). The $E_{leak} - g_{leak}$ branch corresponds to our $E_m - g_m$ branch in this work; the two gated channels g_e and g_i represent excitatory and inhibitory lateral geniculate nucleus (LGN) contributions, respectively; and the gated channel g_{shunt} represents lateral interaction within the visual cortex. The steady-state value of membrane potential V is calculated as $V = I_d/g$, with

$$\begin{aligned} I_d &= g_e E_e + g_i E_i + g_{shunt} E_{shunt} + g_{leak} E_{leak}, \\ g &= g_e + g_i + g_{shunt} + g_{leak}. \end{aligned}$$

It was postulated (see Carandini *et al* 1994) that g_e and g_i act as "linear synaptic conductances" and g_{shunt} as "normalization synaptic conductance". By setting

$$g_i + g_e + g_{leak} = const, \quad (18)$$

$$E_{shunt} = 0, \quad (19)$$

the membrane potential V can be approximated as $V \approx (g_e E_e + g_i E_i + const)/(g_{shunt} + const)$, which effectively states that the linear summation $g_e E_e + g_i E_i$ of LGN inputs is divided by pooled cortical activity (the g_{shunt} term).

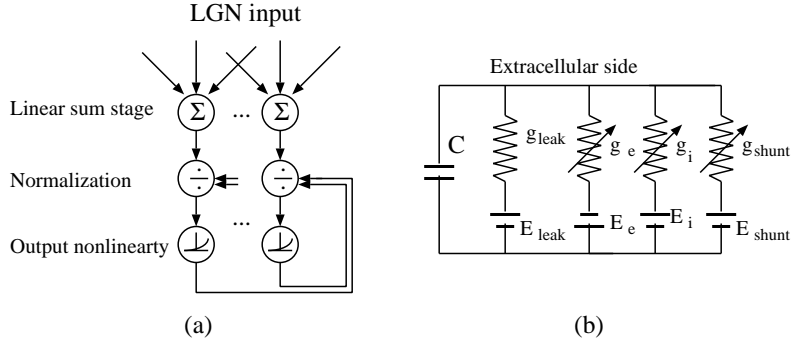


Figure 9: Heeger normalization. (a) Diagram of the normalization model. (b) Equivalent circuit model used by Carandini *et al* to explain the membrane mechanism of normalization (adapted from [1]).

This model is obviously an important generalization to the linear model and can explain a variety of physiological phenomena (Heeger 1992, 1993). However, there are some difficulties in proposing biologically plausible implementation for the two key assumptions (18) and (19). First, the setting (18) requires that both g_e and g_i refer to the LGN inputs. As there has been no evidence for direct thalamocortical inhibition, the g_i term was postulated to come indirectly through other cortical cells (Carandini and Heeger 1994). If this is the case, however, the g_i term should also contribute to the divisor because it contribute to the pooled cortical activity. Secondly, as conductances are non-negative, it is not plain to see how g_i and g_e trade off against one another. Thirdly, the setting (19) implies that the contribution of cortical activity is purely inhibitory, which contradicts to the fact that both excitatory and inhibitory cortico-cortical interactions are experienced by cortical cells.

We show that the Heeger normalization can be accounted for in terms of our rational function model. Consider a cortical cell. For the ease of comparison with their results we omit all axial resistances in the general model and set $E_m = 0$. In this case we are dealing with one spatial summation value only. Letting it be x , we have

$$x \approx \frac{\sum_j E_j w_j^* O(x_j)}{\sum_j [g_m + w_j^* O(x_j)]}.$$

Suppose that the input domain is divided into two non-overlapping clusters such that

$$x \approx \frac{\sum_k^K E_k w_k^* O(x_k) + \sum_l^L E_l w_l^* O(x_l)}{\sum_k^K [g_m + w_k^* O(x_k)] + \sum_l^L [g_m + w_l^* O(x_l)]}$$

where the indices k and l never coincide. If the following conditions hold:

$$\sum_k^K E_k w_k^* O(x_k) \gg \sum_l^L E_l w_l^* O(x_l), \quad (20)$$

$$\sum_k^K w_k^* O(x_k) \ll \sum_l^L w_l^* O(x_l), \quad (21)$$

we have

$$x \approx \frac{\sum_k^K E_k w_k^* O(x_k)}{g_m L + \sum_l^L w_l^* O(x_l)}. \quad (22)$$

If we explain cluster K as the input from the LGN, group L as the pooled cortical activity, then relation (22) restates the normalization model given by Heeger *et al*. The constant $g_m L$ in the divisor corresponds to Heeger's *semisaturation constant* (Heeger 1992, 1993).

Since the LGN inputs are considered all excitatory, $E_k \geq 0$ for all k and so the sum $\sum_k^K E_k w_k^* O(x_k)$ always adds up. However, as cortico-cortical interactions can be both excitatory ($E_l \geq 0$) and inhibitory ($E_l \leq 0$), it

is plausible that many terms in the sum $\sum_i^L E_i w_i^* O(x_i)$ cancel each other. As a result, the condition (20) can be easily satisfied by a large number of w^* settings. On the other hand, the relation (21) can be met if the cortico-cortical synapses made on a cortical cell dominate the synapses made by LGN afferents.

5 Discussion

From the weighted-averaging rule to the ration function model Distinguishing the concept of patch electromotive potential from the concept of spatial summation at a given patch provides a starting point to derive a closed-form model for spatial summation. The weighted-averaging model (4) discloses a hidden relation between these two concepts. From the computational point of view, this model basically states that spatial summation is not a simple accumulation, nor a linear weighted summation, but a nonlinear weighted-average of individual local patch potentials. This nonlinearity lies in that the weighting factors G_{ij} ($j = 1, 2, \dots$) in (4) are not constant coefficients but increasing functions of g_j 's (see (3)). As a result, with a constant total conductance ($\sum_j G_{ij} = \text{const.}$) a larger g_j results in not only a greater patch contribution V_j^m but also a greater weighting factor G_{ij} .

Weighted-averaging seems to be a universal rule in a membrane structure with parallel conductive pathways. We have seen that the calculations of resting potential (see (1)), of patch electromotive potential (see (2)), and of spatial summation (see (4)), all follow the weighted-averaging rule. These three weighted-averaging operations form a hierarchy of observation levels: single channels, single patches, and the whole membrane. However, when the relation of gated channels and spatial summations is concerned, we are dealing with a new, composite function relation: substituting the weighted-average (2) into the weighted-average (4) results in (5) which is no longer a weighted-average (this seems to be a contradiction to that a weighted-average of weighted-average is still a weighted-average). This can be explained by the fact that (4) is a nonlinear weighted-average: both the weighted quantities V_j^m and the weighting factors G_{ij} ($j = 1, 2, \dots$) are functions of g_j 's. This relation is depicted in the diagram in Fig.10.

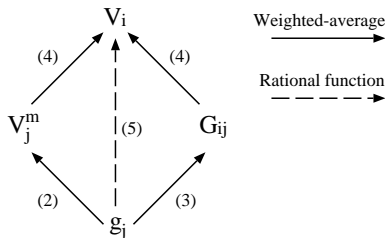


Figure 10: Functional relations among the gated conductances g_j , the patch electromotive potential V_j^m , the inter-patch conductance G_{ij} , and the spatial summation V_i . Numbers with parenthesis refer to equation numbers in the text.

Functional significance of axial resistances The distinction of spatial summation from patch electromotive potential is made possible due to the existence of membrane electrical activity in the perpendicular cross-membrane and tangential-membrane directions. Tangential-membrane activity is mediated by axial resistances. Traditionally, the role played by axial resistances is considered negative: they are thought to be responsible for the decay of activity (a patch electromotive potential of order $10mV$ may contribute only $0.1mV$ to a spatial summation) in the course of spatial summation (as an example, the square of *length constant* λ in the cable theory is proportional to $1/r_a$). However, as we have seen in this work, the influence of axial resistances on spatial summation is subtle. In the case of two patches with opposite polarities, a large axial resistance can block the influence of the inhibitory patch on the excitatory patch and *vice versa*. This helps the spatial summation at the excitatory patch whereas dishelps the other. In the case of several excitatory patches, a large axial resistance blocks the isopolar neighbor shunting, which helps to increase the spatial summation at the the most active patches.

Functional significance of isopolar neighbor shunting In this phenomenon, for several closely-sited, isopolar patches, the spatial summation at a given patch would suffer a remarkable loss of magnitude if only a few (including itself) gated conductances are active while most of others are much less active. One physiological

implication of this is that meaningful afferents to a neuron have to coincide each other in order to produce a significant spatial summation. In contrast, meaningless, spontaneous signals could be effectively masked off through the means of isopolar neighbor shunting. For single neuron computation, two excitatory, closely-sited clusters can ‘inhibit’ each other through isopolar neighbor shunting. In this case, if one afferent cluster needs to inhibit the other, it simply keeps silent (not-to-incorporate), and has not to employ some intermediate, inhibitory cells.

Functional significance of spatial summation There has been an increasing collection of observations which support the idea that neuronal spatial summation may mean more than merely the action potential triggering (Koch and Poggio 1983; Segev and Rall 1988; Mel 1994). Based on the rational model (5), an extension to the conceptual scope of neuronal spatial summation can be suggested: it does not only refer exclusively to the activity accumulation effect at the axon hillock, with the functional significance of summing up individual synaptic signals to overcome the firing threshold. Instead, for every patch on the membrane a local spatial summation value can be observed and is defined by (5). Neglecting temporal summation effects, single neuron computation is completely captured by the distribution of those spatial summation values. Thus, spatial summation affords both the ‘classical’ function of action potential triggering and the other functions which were not considered ‘classical’, such as masking certain afferents, normalizing a cell’s response, or those dendritic functions (Koch and Poggio 1983; Segev and Rall 1988; Mel 1994).

Regarding to information processing, the rational function model (12) suggests that single cortical neurons might behave as *rational approximators*. Since there are a remarkable number of free parameters in the general model (12), it is reasonable to expect more complicated computational functions in the proposed model than what can be achieved by neuronal polynomial approximators (Poggio and Girosi 1990; Dubin and Rumelhart 1990; Mel and Koch 1990).

6 Conclusion

In this work, a closed-form rational function model of spatial summation is derived based on membrane equivalent circuit models. We have shown that tangential-membrane activity plays an important role in neuronal spatial summation, and that single neuron computation can be an intrinsic, universal nature of the general membrane structure with parallel conductive channels. The nonlinear, rational function model of neuronal interaction proposes that single neurons be rational approximators.

Some improvements on the present work are expected in the near future. As this work is focused on a general model of spatial summation, we did not closely match the general model to neurophysiological experimental data. By taking the morphological and physiological features of various cortical neurons into consideration, more biologically realistic models can be expected. Besides, we have seen that single neurons can effectively perform divisions. Biologically plausible implementation of single-neuron multiplication is to be investigated. Finally, our present model of spatial summation is not a complete model for neuronal integration since temporal summation is not considered. A general, closed-form model for neuronal integration will be available shortly.

References

- [1] Carandini, M. and Heeger, D. 1994. Summation and division by neurons in primate visual cortex, *Science* **264**:1333-1336.
- [2] Dubin, R. and Rumelhart, D.E. 1990. Product units: a computationally powerful and biologically plausible extension to backpropagation networks. *Neural Computation* **1**, 133-142.
- [3] Heeger, D. 1993. Modeling single-cell direction selectivity with normalized, half-squared, linear operators, *J. Neurophysiol.* **70**:1885-1898.
- [4] Heeger, D. 1992. Normalization of cell responses in cat striate cortex, *Visual Neuroscience* **9**:181-197.
- [5] Hodgkin, A.L. 1964. *The Conduction of the Nervous Impulse*. Thomas, Springfield, Ill.
- [6] Hubel, D. and Wiesel, T. 1962. Receptive fields, binocular interaction, and functional architecture in the cat’s visual cortex. *Journal of Physiology (London)* **160**:106-154.

- [7] Jack, J. 1979. An introduction to linear cable theory. In em The Neurosciences: Fourth Study Program. F.O. Schmitt and F.G. Worden, eds., pp.423-437. MIT Press, Cambridge, Mass.
- [8] Jack, J., Noble, D., and Tsien, R.W. 1975. *Electric Current Flow in Excitable Cells*. Clarendon Press, Oxford.
- [9] Kandel, E.R., Schwartz J.H. & Jessell, T.M. eds. 1991. *Principles of Neural Science*, 3rd edition, Elsevier, New York.
- [10] Koch, C. and Poggio, T. 1983. A theoretical analysis of electrical properties of spines. *Proc. R. Soc. Lond. B* **218**, 455-477.
- [11] Koch, C., Poggio, T., and Torre, V. 1983. Nonlinear interaction in a dendritic tree: localization, timing and role of information processing. *Proc. Natl. Acad. Sci. U.S.A.* **80**, 2799-2802.
- [12] Mel, B.W. 1994. Information processing in dendritic trees. *Neural Computation* **6**, 1031-1085.
- [13] Mel, B.W., and Koch C. 1990. Sigma-pi learning: On radial basis functions and cortical associative learning. In *Advances in Neural Information Processing Systems*, D.S. Touretzky, ed., Vol.2, pp.474-481. Morgan Kaufmann, San Mateo, CA.
- [14] Poggio, T. and Girosi, F. 1990. Regularization algorithms for learning that are equivalent to multilayer networks, *Science* **247**, 978-982.
- [15] Rall, W. 1964. Theoretical significance of dendritic trees for neuronal input-output relations. In *Exp. Neurology* **2**:503-532, R.F. Reiss ed.
- [16] Segev, I., Fleshman, J.W., and Burke R.E. 1989. Compartmental models of complex neurons. In *Methods in Neuronal Modeling*, C. Koch and I. Segev eds., pp.63-96. MIT Press, Cambridge, Mass.
- [17] Segev, I., and Rall, W. 1988. Computational study of an excitable dendritic spine. *J. Neurophysiol.* **60**, 499-523.
- [18] Shepherd, G.M., and Brayton, R.K. 1987. Logic operations are properties of computer-simulated interactions between excitable dendritic spines. *Neuroscience* **21**, 151-166.
- [19] Zador, A.M., Claiborne, B.J., and Brown, T.J. 1992. Nonlinear pattern separation in single hippocampal neurons with active dendritic membrane. In *Advances in Neural Information Processing Systems*, J. Moody, S. Hanson, and R. Lippmann, eds., Vol.4, pp.51-58. Morgan Kaufmann, San Mateo, CA.